Rate constants for proteins binding to substrates with multiple binding sites using a generalized forward flux sampling expression

Vijaykumar, A.; ten Wolde, P.R.; Bolhuis, P.G.

DOI
10.1063/1.5012854

Publication date
2018

Document Version
Final published version

Published in
Journal of Chemical Physics

Rate constants for proteins binding to substrates with multiple binding sites using a generalized forward flux sampling expression

Adithya Vijaykumar,[1,2] Pieter Rein ten Wolde,[1,a)] and Peter G. Bolhuis[2,b)]
[1]*FOM Institute AMOLF, Science Park 104, 1098 XG Amsterdam, The Netherlands*
[2]*van't Hoff Institute for Molecular Sciences, University of Amsterdam, P.O. Box 94157, 1090 GD Amsterdam, The Netherlands*

(Received 8 November 2017; accepted 29 January 2018; published online 26 March 2018)

To predict the response of a biochemical system, knowledge of the intrinsic and effective rate constants of proteins is crucial. The experimentally accessible effective rate constant for association can be decomposed in a diffusion-limited rate at which proteins come into contact and an intrinsic association rate at which the proteins in contact truly bind. Reversely, when dissociating, bound proteins first separate into a contact pair with an intrinsic dissociation rate, before moving away by diffusion. While microscopic expressions exist that enable the calculation of the intrinsic and effective rate constants by conducting a single rare event simulation of the protein dissociation reaction, these expressions are only valid when the substrate has just one binding site. If the substrate has multiple binding sites, a bound enzyme can, besides dissociating into the bulk, also hop to another binding site. Calculating transition rate constants between multiple states with forward flux sampling requires a generalized rate expression. We present this expression here and use it to derive explicit expressions for all intrinsic and effective rate constants involving binding to multiple states, including rebinding. We illustrate our approach by computing the intrinsic and effective association, dissociation, and hopping rate constants for a system in which a patchy particle model enzyme binds to a substrate with two binding sites. We find that these rate constants increase as a function of the rotational diffusion constant of the particles. The hopping rate constant decreases as a function of the distance between the binding sites. Finally, we find that blocking one of the binding sites enhances both association and dissociation rate constants. Our approach and results are important for understanding and modeling association reactions in enzyme-substrate systems and other patchy particle systems and open the way for large multiscale simulations of such systems. *Published by AIP Publishing.*
https://doi.org/10.1063/1.5012854

I. INTRODUCTION

Unimolecular and bimolecular reactions are the building blocks of many complex processes in biology, chemistry, and soft condensed matter. Knowledge of equilibrium constants is imperative to evaluate the importance of biological reactions like DNA-protein binding,[1] receptor-ligand binding, and enzyme-substrate binding.[2–4] However, many biological processes are controlled not only by the equilibrium constant but also by the absolute rates themselves. The rate constants determine the response time of living cells, which is vital for the fitness of the organism in a fluctuating environment. Knowledge of the individual rates is also important in the field of drug development, i.e., for setting the optimal dosage and for improving drug efficacy.[5] Also discrimination by our immune system is believed to depend on the dissociation rate, rather than the equilibrium constant.[6]

Experimentally measured association and dissociation rates are typically effective rates.[2,7,8] These effective rates describe a two-step process. During association, particles come into contact via diffusion and bind with a rate depending on the intrinsic association rate constant. When dissociating, a bound particle pair separates with an intrinsic dissociation rate, after which the particles diffuse away from each other. Agmon and Szabo[7] and Berg and von Hippel[8] derived expressions for the effective binding and unbinding rate constants in terms of the diffusion constants, cross sections, interaction potentials, and intrinsic rate constants. However, they assume that the intrinsic rate constants are known *a priori*. To compute effective rate constants in computer simulations, one can use the simulation methods developed by Northrup and Erickson[9] and Zhou.[10] However, these methods do not yield the intrinsic rate constants.

In many cases, not only the effective rate constants are necessary for describing the dynamics of the system but also the intrinsic rate constants. A particularly striking example is the class of cellular systems that is based on multi-site protein modification. Many substrates possess multiple chemical modification sites. It has long been known that the response of the system strongly depends on whether the enzyme modifies the sites according to a distributive or a processive mechanism.[11–13] In a distributive scheme, after modifying the first site, the enzyme needs to dissociate from the site before it can rebind and modify the next site. In a processive scheme,

a)Electronic mail: tenwolde@amolf.nl
b)Electronic mail: p.g.bolhuis@uva.nl

the enzyme remains bound to the substrate in between the modification of the two sites. In a pseudo-processive scheme, an enzyme molecule does dissociate from the first site but then rebinds and modifies the other site before another enzyme molecule from the bulk does, yielding the same response as that of a purely processive scheme.[14–16] Rebinding at the molecular scale can thus change the response from a distributive scheme to an effectively processive one. This can qualitatively change the behavior of the system at the macroscopic scale, leading to the loss of bistability and ultrasensitivity.[14–16] In addition, these enzyme-substrate rebindings can have important implications for proofreading.[17] Another class of problems where the microscopic dynamics is important is receptor-ligand binding. The microscopic dynamics of ligand binding to and hopping between multiple receptors affects the accuracy of chemical sensing, both in living cells and in artificial sensors.[18–22] In all these examples, the dynamics of the system cannot be described by effective rate constants: knowledge of the diffusion constants, cross sections, and intrinsic rate constants for hopping, association, and dissociation is required. Since these systems are difficult to analyze analytically, they are often studied by computer simulations via algorithms that can propagate the system at the particle level, using cross sections, diffusion constants, and intrinsic rate constants as input parameters.[14,23–27]

In a previous paper,[28] we derived explicit microscopic expressions for the intrinsic and effective rate constants, and we presented a numerical approach that makes it possible to compute all rates—the effective and intrinsic association and dissociation rates—in one rare-event simulation of the dissociation process. We showed how this scheme can be applied to not only isotropic but also anisotropic particles. However, the technique that we presented was limited to only one site on each particle. It therefore did not allow for the computation of the rate constant for hopping between two sites on the same particle. This is a drawback since pseudo-processivity relies on the hopping of a dissociated particle from one site to the next: a particle dissociates, and instead of diffusing into the bulk, it rebinds, i.e., hops, to the other site.

Here, we extend the approach of Ref. 28 to enable the computation of not only the effective and intrinsic association and dissociation rate constants in one rare-event simulation but also that of the hopping rate constant. The rare-event simulation technique could, for example, be Transition Interface Sampling (TIS)[29] or Forward Flux Sampling (FFS).[30,31] Here we use the latter technique. However, FFS has so far mostly been used for computing rate constants for transitions between two states, rather than between multiple states. We therefore first generalize the canonical FFS expression, which is based on that of TIS,[29,30] so that it allows the computation of rate constants for transitions among multiple states. This expression is general and can also be used in other contexts than the one considered here.

We then apply our scheme to study the association and dissociation of an enzyme to and from a substrate with two enzyme-binding sites as well as the hopping of the enzyme between the two binding sites. We study these rate constants as a function of the distance (angle) between the two sites.

As a simple approximation to the complex anisotropic protein-protein interaction, we employ the so-called patchy particle model in which the binding sites are modeled as patchy interactions between otherwise isotropically interacting spherical particles. Such patchy particles not only can model globular proteins[32–37] but also play a role in the design and modeling of novel self-assembled materials, for instance, in colloidal particles with specific binding sites.[38–40] The multivalency of the particles and the nature of the patches can alter the relaxation pathways to the most stable state and can induce higher order phases.[41,42] Knowledge of the association kinetics of such systems enables the understanding and improved design of complex colloidal self-assembly.[43,44]

As the interaction potential is anisotropic, particles undergo both translational and orientational diffusion. We therefore also study the rate constants as a function of the orientational diffusion constant of the particles. Here, we capitalize on the observation that in a crowded environment the orientational diffusion constant can be varied independently of the translational diffusion constant, by varying the nature and the concentration of the crowders.[33,45,46]

We find that all rate constants increase with the orientational diffusion constant, with the hopping rate constant showing the strongest dependence on the orientational diffusion constant and the association rate the weakest. Moreover, we find, as expected, that the hopping rate constant decreases as the angle between the patches increases, while the association and dissociation rate constants are less affected by patch separation.

In a real system, hopping might be blocked by another enzyme bound to the substrate. To investigate the effect on the association and dissociation rate constants, we compare the scenario of a substrate with two sites with a scheme in which the substrate has one site and with one in which one of the two sites is blocked by an enzyme molecule. We find that the rate constants for binding to *one specific* site out of the two sites are smaller than the rate of binding to a substrate with one site. This seemingly counter-intuitive result is a result of the fact that the processes of binding to the two respective sites are not independent: In binding to one specific site, the other site effectively acts as a trap, reducing the association rate constant.[47] On the other hand, the two sites together have a larger effective cross section than a single-site substrate, such that the reduction in the association rate constant is less than a factor of two; or put differently, the rate constant of binding to either patch is larger than the rate constant of binding to a substrate with one site only. As expected from microscopic reversibility, the other site also acts as a trap on the dissociation pathway, reducing the dissociation rate constant.

These results show that the intrinsic association, hopping, and dissociation rate constants can be important for describing the dynamics of the system. Moreover, they emphasize that the binding and unbinding kinetics can strongly be affected by adjacent binding patches and the orientational dynamics of the molecules.

The remainder of the paper is as follows. In Sec. II A, we derive the general FFS expression, followed by a derivation of the intrinsic rate constant expressions for in Sec. II B. We discuss the results in Sec. III. We end with concluding remarks.

II. METHODS

A. Rate constants from forward flux sampling when two states are not separated by all interfaces

Dissociation of anisotropic particles is often a rare event. In order to simulate such rare event kinetics with minimal computational effort, an efficient rare event simulation technique such as Forward Flux Sampling (FFS)[30,31] or Transition Interface Sampling (TIS)[29] is necessary. Here, we use FFS to simulate the dissociation reaction.

The crux of FFS is to drive the system from one state to another in a ratchet-like manner by capitalizing on those fluctuations that happen to move the system in the right direction. To capitalize on these fluctuations, FFS uses a series of interfaces between the initial and final states. These interfaces make it possible to store configurations along trajectories that have progressed in the direction of the final state. While FFS is typically employed for computing rate constants for transition between two states, here we present a new expression, which may prove useful for computing rate constants for transitions between multiple states.

Figure 1 illustrates the scheme for a scenario of three metastable states: A, B, and U. These states are defined in terms of an order parameter λ. Here, we are interested in the transition rate constants k_{AB} and k_{AU}. While the expressions that we will derive below are generic and can be generalized to any system consisting of multiple metastable states, it is illuminating to consider the concrete scenario in which state A corresponds to an enzyme molecule that is bound to patch A of a substrate molecule, state B as the enzyme molecule being bound to patch B of the substrate molecule, and state U as the state in which the enzyme and substrate molecules are unbound. The dissociation rate constant k_{AU} is then defined as the rate constant for dissociating from patch A into the unbound state U while not visiting state B; the ensemble of transition paths that corresponds to k_{AU} thus contains trajectories that start from A and end at U yet do not visit B. By contrast, the hopping rate constant k_{AB} is

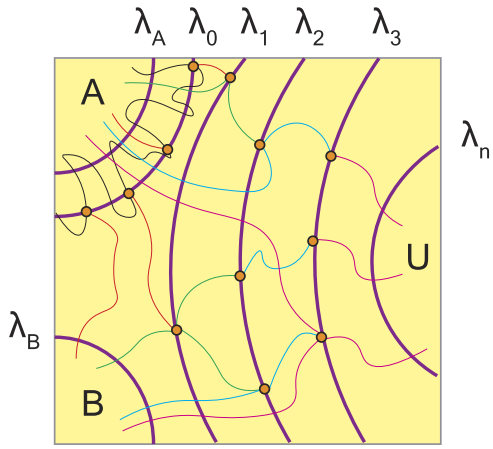

FIG. 1. Illustration of the possible trajectories starting from state A and ending either in state B or state U and the interfaces $\lambda_0, \ldots, \lambda_{n-1}$ used in the FFS simulation. A trajectory starting at A and terminating at B need not pass through all these interfaces, but a trajectory starting at A and terminating at U has to pass through all the interfaces. Note that the interfaces are defined by a single parameter λ. The 2D projection is purely to illustrate the effect of multiple states.

defined as the rate constant at which the enzyme molecule dissociates from patch A and then diffuses to and rebinds to patch B. Importantly, the transition path ensemble that corresponds to this hopping rate constant contains not only trajectories that directly go from A to B but also trajectories that have significantly progressed in the direction of U before arriving at B. Here, we will derive the expressions that make it possible to compute the transition rates constant k_{AB} and k_{AU} in an FFS simulation.

As Fig. 1 illustrates, the interfaces $\lambda_0, \lambda_1, \ldots, \lambda_{n-1}, \lambda_n$ are defined such that all trajectories of the transition path ensemble corresponding to k_{AU} necessarily cross all interfaces $\lambda_0, \lambda_1, \ldots, \lambda_{n-1}, \lambda_n$. As a result, the expression for k_{AU} is based on the conventional TIS expression used also in FFS,[29,30]

$$k_{AU} = \Phi_0 \prod_{i=0}^{n-1} P(\lambda_{i+1}|\lambda_i). \tag{1}$$

Here, λ_i define the intermediate interfaces between state A and state U, as illustrated in Fig. 1. The quantity Φ_0 is the flux of trajectories that start from A and then cross interface λ_0, while $P(\lambda_{i+1}|\lambda_i)$ is the conditional probability that a trajectory which comes from A and crosses λ_i for the first time will subsequently reach λ_{i+1} instead of returning to A or progressing to B. In an FFS simulation, one thus first performs a brute-force simulation in state A; this makes it possible not only to compute the flux Φ_0 through the first interface λ_0 but also to generate an ensemble of points at λ_0. In the next step, one then randomly picks a configuration from this ensemble of points at λ_0 and launches and propagates a trajectory from this configuration until it either arrives at λ_1, returns to A, or arrives at B; by iterating this a number of times, one obtains not only an ensemble of configurations at λ_1 but also $P(\lambda_1|\lambda_0)$ as the fraction of trajectories that reach λ_1. This procedure is then repeated for all the subsequent interfaces, yielding $P(\lambda_{i+1}|\lambda_i)$ for all interfaces λ_i.

In contrast to the trajectories of the AU transition path ensemble, the trajectories of the AB path ensemble do not necessarily cross all interfaces $\lambda_0, \lambda_1, \ldots, \lambda_{n-1}, \lambda_n$. Some paths directly go from A to B, while other trajectories cross λ_1 and perhaps even $\lambda_i > \lambda_1$, before proceeding to B. All these excursions must be accounted for to calculate the transition rate constant from A to B. This means that Eq. (1) cannot be used to compute k_{AB}. A general expression for the transition rate constant between two states, where the trajectories start at A and end at B yet do not necessarily cross all intermediate interfaces, is given by

$$\begin{aligned} k_{AB} = \Phi_0 \Big[& P(\lambda_B|\lambda_0) + P(\lambda_1|\lambda_0)P(\lambda_B|\lambda_1) \\ & + P(\lambda_1|\lambda_0)P(\lambda_2|\lambda_1)P(\lambda_B|\lambda_2) + \cdots \\ & + P(\lambda_1|\lambda_0), \ldots, P(\lambda_{n-1}|\lambda_{n-2})P(\lambda_n|\lambda_{n-1})P(\lambda_B|\lambda_n) \Big] \\ = \Phi_0 & \sum_{i=0}^{n} P(\lambda_B|\lambda_i)P(\lambda_i|\lambda_0). \end{aligned} \tag{2}$$

Here, $P(\lambda_B|\lambda_i)$ is the probability that a trajectory which is launched at interface λ_i arrives at B before reaching either A or λ_{i+1}, while $P(\lambda_{i+1}|\lambda_i)$ is, as before, the probability that

a trajectory which is fired at λ_i arrives at λ_{i+1} before reaching either A or B. In the last line, we summed the expression realizing that $P(\lambda_i|\lambda_0) = \prod_{j=0}^{i-1} P(\lambda_{j+1}|\lambda_j)$.

Equation (2) is a generic equation to calculate the transition rate constant between two states. Equation (2) reduces to Eq. (1) when the trajectories from the initial state have to pass through all the interfaces to reach the final state. Note that the expression is also applicable to the case of more than two states.

We note that a similar situation of stable states nested between interfaces occurs in multiple state TIS and single replica exchange TIS, which was treated in Refs. 33, 44, 47, and 48.

B. Effective and intrinsic rate constants for two binding sites

We now apply the generic equation (2) to the specific case of an enzyme-substrate association-dissociation reaction, where the enzyme has one binding site, while the substrate has two binding sites. We will first discuss the details of the path ensembles that correspond to each of the rate constants.

The intrinsic dissociation rate constants for the enzyme initially bound at patch A, $k_{\mathrm{d}}^{A}(\sigma)$, involve counting the trajectories that start from A and reach σ without reaching patch B (see Fig. 2 for a graphical illustration). Similarly, the effective dissociation rate constant for the enzyme starting at patch A, k_{off}^{A}, takes into account all trajectories starting at A and going up to infinity, without visiting patch B. The effective association constant of an enzyme to bind to patch A, k_{on}^{A}, corresponds to trajectories that start at infinity and terminate at patch A without first visiting B, while the intrinsic association rate constant $k_{\mathrm{a}}^{A}(\sigma)$ corresponds to trajectories that start at the σ-interface and terminate at patch A without first visiting B. The intrinsic rate constant of hopping from patch A to B, $k_{\mathrm{hop}}^{AB}(\sigma)$, corresponds to trajectories that start from patch A and end at patch B, without first visiting the σ-interface, while the effective rate constant of hopping from patch A to patch B, $k_{\mathrm{effHop}}^{AB}(\sigma)$, corresponds to trajectories that start from patch A and end at patch B, without diffusing to infinity (however, they may cross the σ interface). We can similarly define the ensemble of trajectories that define the rate constants for associating to and dissociating from patch B. We emphasize that while the intrinsic rate constants depend on the definition of σ, the effective rate constants do not.

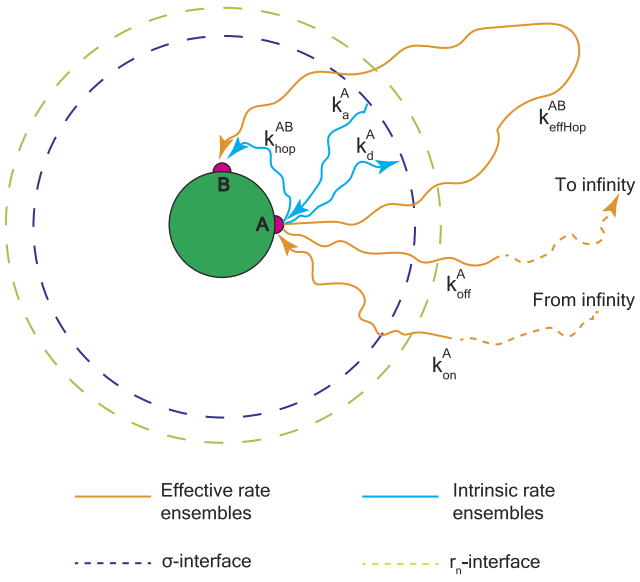

FIG. 2. The path ensembles contributing to each rate constant. The substrate has two patches A and B, and when the particle diffuses to infinity, it is in the unbound state. All rates are calculated with respect to the patch A, i.e., the rate constant of binding to patch A or the rate constant of unbinding from patch A. σ is the interface where the intrinsic rate constants are measured, and r_{n} is an interface beyond σ.

We will now show how from a single FFS simulation of a dissociation reaction from patch A both the intrinsic and effective dissociation rate constants and the intrinsic and effective hopping and association rate constants can be computed. The intrinsic dissociation rate constant at the σ-interface is given by

$$k_{\mathrm{d}}^{A}(\sigma) = \Phi_0 P(\sigma|r_0), \tag{3}$$

where, as before, Φ_0 is the flux across the first FFS interface r_0 and $P(\sigma|r_0)$ is the probability that an enzyme starting at this first interface reaches the σ-interface before binding to either patch and can be computed using Eq. (1). The effective dissociation constant can be similarly expressed as

$$k_{\mathrm{off}}^{A} = \Phi_0 P(\sigma|r_0) P(\infty|\sigma) = k_{\mathrm{d}}^{\mathrm{A}}(\sigma) P(\infty|\sigma), \tag{4}$$

where $P(\infty|\sigma)$ is the probability that a trajectory which has reached σ, escapes to infinity, i.e., dissociates, before it associates with either patch A or patch B.

The intrinsic hopping rate constant, given that the enzyme starts at patch A, is given by

$$k_{\mathrm{hop}}^{\mathrm{AB}} = \Phi_0 P(B|r_0), \tag{5}$$

where $P(B|r_0)$ is the probability that the enzyme, starting at patch A, associates with patch B before it arrives at σ.

The effective hopping rate constant, given that the enzyme starts bound to patch A, is given by Eq. (2). Taking for simplicity only three interfaces ($n = 1$) located at $\lambda_0 \equiv r_0$, $\lambda_1 \equiv \sigma$, and $\lambda_B \equiv B$, this expression becomes

$$k_{\mathrm{effHop}}^{AB} = \Phi_0 \left[P(B|r_0) + P(\sigma|r_0) P(B|\sigma)\right], \tag{6}$$

where $P(\sigma|r_0)$ is the probability of the enzyme starting at the first interface r_0, subsequently reaching the σ-interface before binding to either patch. $P(B|\sigma)$ is the probability that the enzyme, starting at σ, reaches B before it either escapes (i.e., dissociates) or reaches A; the path ensemble corresponding to this effective hopping rate constant does include, however, trajectories that progress (significantly) beyond the σ interface. In a full FFS simulation employing multiple (n) interfaces, $P(B|r_0)$ and $P(\sigma|r_0)$ are replaced by the full summation over n as in Eq. (2).

To see how all the rate constants (intrinsic/effective association, dissociation, and hopping rate constant) can be obtained from one single FFS simulation of a dissociation reaction, it is instructive to imagine that starting from the bound state A, we have generated N configurations at interface σ. These configurations are thus distributed over the σ surface according to the distribution as obtained from an FFS dissociation simulation starting from patch A.

Of the N trajectories at interface σ, $N_{\sigma\to B}$ progress (on average) to B, $N_{\sigma\to A}$ return to A, and $N_{\sigma\to\infty}$ dissociate, i.e., escape to infinity: $N = N_{\sigma\to B} + N_{\sigma\to A} + N_{\sigma\to\infty}$. In the limit of $N\to\infty$, we can define the probabilities $P(B|\sigma) = N_{\sigma\to B}/N$, $P(A|\sigma) = N_{\sigma\to A}/N$, $P(\infty|\sigma) = N_{\sigma\to\infty}/N$. For a finite number of sampled trajectories, the trajectory fractions become approximations of these probabilities. We can then write

$$\begin{aligned} P(B|\sigma) &= \frac{P(B|\sigma)}{P(A|\sigma)+P(B|\sigma)}(P(A|\sigma)+P(B|\sigma)) \\ &= \frac{P(B|\sigma)}{P(A|\sigma)+P(B|\sigma)}(1-P(\infty|\sigma)) \\ &= \alpha(1-P(\infty|\sigma)), \end{aligned} \tag{7}$$

where we have defined

$$\alpha \equiv \frac{P(B|\sigma)}{P(A|\sigma)+P(B|\sigma)} \tag{8}$$

and made use of the fact that $P(A|\sigma)+P(B|\sigma)+P(\infty|\sigma)\,) = 1$, and we have introduced α as a "splitting probability" for trajectories from σ arriving at B versus A. To compute $P(\infty|\sigma)$ in a brute-force manner, one would have to generate extremely long trajectories because there is always a small but finite probability that an enzyme molecule which has diffused far away and deep into the bulk will return to the substrate molecule. To mitigate this problem, we put, following our earlier work,[28] an interface at a position $r_\mathrm{n} > \sigma$. As we will show below, this extra interface makes it possible to efficiently compute $P(\infty|\sigma)$. Moreover, the probability $P(B|\sigma)$ for trajectories that move from σ to B is then given by the sum of the probability $P_\mathrm{dir}(B|\sigma)$ of trajectories that directly go from σ to B without first visiting r_n and the probability $P_{r_\mathrm{n}}(B|\sigma)$ for those that first visit r_n and then proceed to B,

$$\begin{aligned} P(B|\sigma) &= P_\mathrm{dir}(B|\sigma) + P_{r_\mathrm{n}}(B|\sigma) \\ &= \alpha_\mathrm{dir}\,(P_\mathrm{dir}(A|\sigma)+P_\mathrm{dir}(B|\sigma)) \\ &\quad + \alpha_{r_\mathrm{n}}(P_{r_\mathrm{n}}(A|\sigma)+P_{r_\mathrm{n}}(B|\sigma)) \\ &= \alpha_\mathrm{dir}(1-P(r_\mathrm{n}|\sigma)) + \alpha_{r_\mathrm{n}}P(r_\mathrm{n}|\sigma)(1-P(\infty|r_\mathrm{n})). \end{aligned} \tag{9}$$

Here, α_dir and α_{r_n} are, respectively, the splitting probabilities of arriving at A versus B of those trajectories that proceed directly from σ to either A or B and those that arrive at A or B passing via r_n,

$$\alpha_\mathrm{dir} = \frac{P_\mathrm{dir}(B|\sigma)}{P_\mathrm{dir}(A|\sigma)+P_\mathrm{dir}(B|\sigma)}, \tag{10}$$

$$\alpha_{r_\mathrm{n}} = \frac{P_{r_\mathrm{n}}(B|\sigma)}{P_{r_\mathrm{n}}(A|\sigma)+P_{r_\mathrm{n}}(B|\sigma)}. \tag{11}$$

Similarly for the trajectories starting at the σ-interface and reaching A, we can write

$$\begin{aligned} P(A|\sigma) &= (1-\alpha_\mathrm{dir})(1-P(r_\mathrm{n}|\sigma)) \\ &\quad + (1-\alpha_{r_\mathrm{n}})P(r_\mathrm{n}|\sigma)(1-P(\infty|r_\mathrm{n})). \end{aligned} \tag{12}$$

As a sanity check, we can add Eqs. (9) and (12) which gives

$$\begin{aligned} P(A|\sigma)+P(B|\sigma) &= 1-P(r_\mathrm{n}|\sigma)+P(r_\mathrm{n}|\sigma)\,(1-P(\infty|r_\mathrm{n}) \\ &= 1-P(r_\mathrm{n}|\sigma)P(\infty|r_\mathrm{n}) \\ &= 1-P(\infty|\sigma), \end{aligned} \tag{13}$$

which is indeed equal to the probability to observe trajectories that do not escape to infinity and hence bind to either A or B.

Combining Eqs. (8), (9), and (12) yields

$$\alpha = \frac{\alpha_\mathrm{dir}(1-P(r_\mathrm{n}|\sigma)) + \alpha_{r_\mathrm{n}}P(r_\mathrm{n}|\sigma)(1-P(\infty|r_\mathrm{n}))}{1-P(\infty|\sigma)}. \tag{14}$$

The quantities $P(r_\mathrm{n}|\sigma)$, $P(\infty|\sigma)$, and α_dir can be directly obtained from the FFS simulations. Hence, to close the above equation and find $P(B|\sigma)$ [see Eq. (7)], we need an expression for α_{r_n}. Since $P_{r_\mathrm{n}}(B|\sigma)$ is the product of the probability $P(r_\mathrm{n}|\sigma)$ of trajectories going from σ to r_n and the probability $P(B|r_\mathrm{n})$ of subsequently reaching B, the splitting probability α_{r_n} in Eq. (11) is also given by

$$\begin{aligned} \alpha_{r_\mathrm{n}} &= \frac{P_{r_\mathrm{n}}(B|\sigma)}{P_{r_\mathrm{n}}(A|\sigma)+P_{r_\mathrm{n}}(B|\sigma)} \\ &= \frac{P(r_\mathrm{n}|\sigma)P(B|r_\mathrm{n})}{P(r_\mathrm{n}|\sigma)P(A|r_\mathrm{n})+P(r_\mathrm{n}|\sigma)P(B|r_\mathrm{n})} \\ &= \frac{P(B|r_\mathrm{n})}{P(A|r_\mathrm{n})+P(B|r_\mathrm{n})}. \end{aligned} \tag{15}$$

We emphasize that up to this point, no assumption has been made. In particular, the expressions hold for any choice of the location σ, including one that is close to the bound state, which would lead to a non-uniform distribution of configurations at σ. With such a non-uniform distribution, α_{r_n} is likely to be unequal to α_dir, which would make it impossible to close Eq. (14). By contrast, if the distributions at the σ and the r_n interfaces are isotropic, then

$$\frac{P_{r_\mathrm{n}}(B|\sigma)}{P_{r_\mathrm{n}}(A|\sigma)+P_{r_\mathrm{n}}(B|\sigma)} \simeq \frac{P_\mathrm{dir}(B|\sigma)}{P_\mathrm{dir}(A|\sigma)+P_\mathrm{dir}(B|\sigma)}, \tag{16}$$

and, thus,

$$\alpha_{r_\mathrm{n}} = \alpha_\mathrm{dir}. \tag{17}$$

Inserting Eq. (17) in Eq. (14), we find

$$\alpha = \alpha_\mathrm{dir} = \alpha_{r_\mathrm{n}} \equiv \frac{P(B|\sigma)}{P(A|\sigma)+P(B|\sigma)}, \tag{18}$$

which reduces Eq. (7) to

$$P(B|\sigma) = \alpha_\mathrm{dir}(1-P(\infty|\sigma)). \tag{19}$$

Hence the effective hopping rate constant from Eq. (6) reduces to

$$k^{AB}_\mathrm{effHop} = \Phi_0\,[P(B|r_0) + \alpha_\mathrm{dir}P(\sigma|r_0)(1-P(\infty|\sigma))]\,. \tag{20}$$

Note that when A and B are identical patches, then $\alpha = \alpha_\mathrm{dir} = 0.5$. However, in general, this does not need to be the case.

Both the effective dissociation rate constant given by Eq. (4) and the effective hopping rate constant in Eq. (20) require the calculation of the escape probability $P(\infty|\sigma)$. Below, we describe how $P(\infty|\sigma)$ can be obtained efficiently in an FFS simulation. The escape probability, together with the diffusion-limited arrival rate constant $k_D(\sigma)$, makes it possible to define the intrinsic association rate constant,[28]

$$P(\infty|\sigma) = \frac{k_\mathrm{D}(\sigma)}{k_\mathrm{a}^{\mathrm{A}\vee\mathrm{B}}(\sigma)+k_\mathrm{D}(\sigma)}, \tag{21}$$

where $k_a^{A\vee B}$ is the intrinsic rate constant at which a particle at σ binds either A or B. This equation, and hence the intrinsic association rate constant, can, in principle, also be defined for surfaces σ for which the distribution of configurations is not isotropic;[28] yet, the expression for the diffusion-limited arrival rate constant $k_D(\sigma)$ is then, in general, not known. In the case considered here, where the distribution of configurations at σ is isotropic [and σ is (significantly) beyond the cutoff of the potential], the diffusion-limited arrival rate constant is, however, simply given by $k_D(\sigma) = 4\pi\sigma D$, where D is the (sum of the) diffusion constant(s) of the particles. Rearranging the above equation yields the intrinsic rate constant of binding to either A or B,

$$k_a^{A\vee B}(\sigma) = k_D(\sigma)\frac{1 - P(\infty|\sigma)}{P(\infty|\sigma)}. \tag{22}$$

The effective association rate constant of binding to either A or B is given by the diffusion-limited arrival rate constant $k_D(\sigma)$ times the binding probability $(1 - P(\infty|\sigma))$,

$$k_{on}^{A\vee B} = k_D(\sigma)(1 - P(\infty|\sigma)), \tag{23}$$

the effective association rate constant of binding to patch A is

$$k_{on}^{A} = (1 - \alpha)(1 - P(\infty|\sigma))k_D(\sigma), \tag{24}$$

and the intrinsic association rate constant of binding to patch A is given by

$$k_a^{A}(\sigma) = (1 - \alpha)k_a^{A\vee B}(\sigma). \tag{25}$$

Equations (3)–(5), (20), (25), and (24) yield the expressions for the intrinsic and effective dissociation, hopping, and association rate constants. Only one point remains to be addressed, which is how $P(\infty|\sigma)$ can be obtained efficiently in an FFS simulation. To this end, we exploit that the effective rate constant of binding either patch is independent of the location of the effective cross section,[28]

$$k_{on}^{A\vee B}(\sigma) = k_{on}^{A\vee B}(r_n), \tag{26}$$

which means, using Eq. (23), that

$$k_D(\sigma)(1 - P(\infty|\sigma)) = k_D(r_n)(1 - P(\infty|r_n)). \tag{27}$$

$P(\infty|\sigma)$ can be factorized as

$$P(\infty|\sigma) = P(\infty|r_n)P(r_n|\sigma). \tag{28}$$

Solving Eqs. (27) and (28) yields

$$P(\infty|\sigma) = \frac{P(r_n|\sigma)(1 - \Omega)}{1 - \Omega P(r_n|\sigma)}, \tag{29}$$

where $\Omega \equiv k_D(\sigma)/k_D(r_n)$. If the interfaces σ and r_n are beyond the cutoff of the potential, then the particles move by free diffusion. In this case, we can exploit the analytic expression for the diffusion-limited arrival rate constant $k_D(\sigma) = 4\pi\sigma D$ to evaluate all the rate constants.

The above equations hold for a situation in which both A and B are very long lived states so that the association rate constant k_{AU} for binding to A is dominated by the paths that directly proceed from the unbound state to path A, and the paths that visit B do not contribute significantly to k_{AU}. We argue that also in the (mean-field) modeling of biochemical networks, this is the most natural and useful definition of the association rate constant.

C. Particle model and interaction potential

All particles are spherical with an isotropic centre of mass interaction, dressed with one or more sticky spots on their surface called "patches," which allow for highly directional, anisotropic interactions. We use two species of such particles in our simulations, a substrate particle which has two patches and an enzyme particle that has one patch.

The enzyme-substrate pair, in our model, experiences a strong attractive potential, $U_s(r)$, over a narrow band of orientations (see Fig. 3). This specific attraction depends on the distance, r, between the patches, i.e., stronger attraction when the patches are closer. When the patchy particles approach each other, they experience a repulsive potential, $U_{rep}(R)$, which is a function of the center-of-mass distance, R. In addition, particles experience a weak, isotropic, non-specific attraction, $U_{ns}(R)$. The total patch potential reads

$$U_{an}(R, r) = \sum_{i=1}^{n} U_s(r_i) + U_{rep}(R) + U_{ns}(R), \tag{30}$$

where n is the number of patches on the substrate (two in the context of this paper) and r_i are the inter-patch distances between the patch of the enzyme and the ith patch of the substrate. $U_s(r)$, $U_{rep}(R)$, and $U_{ns}(R)$ have the form

$$U_i(x) = \begin{cases} \epsilon_i\left(1 - a_i\left(\frac{x}{\sigma_{an}}\right)^2\right) & \text{if} \quad x < x_i^\star, \\ \epsilon_i b_i\left(\frac{x_i^c}{\sigma_{an}} - \frac{x}{\sigma_{an}}\right)^2 & \text{if} \quad x_i^\star < x < x_i^c, \\ 0 & \text{otherwise}, \end{cases} \tag{31}$$

with $i = \{s, rep, ns\}$, respectively. The overall strength ϵ_i, the length scale $\sigma_{an} = 5$ nm, the stiffness a_i, and the parameter $x_i^\star$, which when combined with a_i determines the range of the potential, are free parameters. Cutoffs x_i^c and smoothing parameters b_i are fixed by requiring continuity and differentiability at $x_i^\star$. In this paper, we use the same parameter settings as in Refs. 28, 49, and 50: $\epsilon_s = 20k_BT$, $a_s = 20$, and $r_{att}^* = 0.1\sigma_{an}$, implying $b_s = 5$ and $r_s^c = 0.5\sigma_{an}$; $\epsilon_{rep} = 100k_BT$, $a_{rep} = 1$, and $R_{rep}^* = 0.85\sigma_{an}$, implying $b_{rep} = 2.6036$ and $R_{rep}^c = 1.1764\sigma_{an}$; and $a_{ns} = 1$ and $R_{ns}^* = 0.85\sigma_{an}$, implying $b_{ns} = 2.6036$ and $R_{ns}^c = 1.1764\sigma_{an}$. ϵ_{ns} is varied from $2k_BT$ to $20k_BT$ with steps of $2k_BT$. When the patches are aligned ($r = R - \sigma_{an}$) and misaligned ($r = R + \sigma_{an}$). When the patches are aligned, particles experience both specific and non-specific attraction, creating a deeper potential well and a stronger bond. When the patches are misaligned, $U_s = 0$, and the particles only experience the weak U_{ns} which results in a shallow potential well and a weaker bond. The non-specific attraction, however, promotes realignment since the particles do not diffuse away immediately.

Particles of the same species, i.e., enzyme-enzyme and substrate-substrate, only have a WCA (Weeks-Chandler Andersen) repulsion based on the centre of mass distance, R.

These parameters were chosen to mimic protein association with dissociation constants on the order of nM to mM.[2,51,52] The length scale $\sigma_{an} = 5$ nm represents a typical diameter for a protein substrate or enzyme. Not only the dissociation constant, corresponding to the ratio of the dissociation and association rate, corresponds to that in many biochemical networks but also the absolute rates themselves,

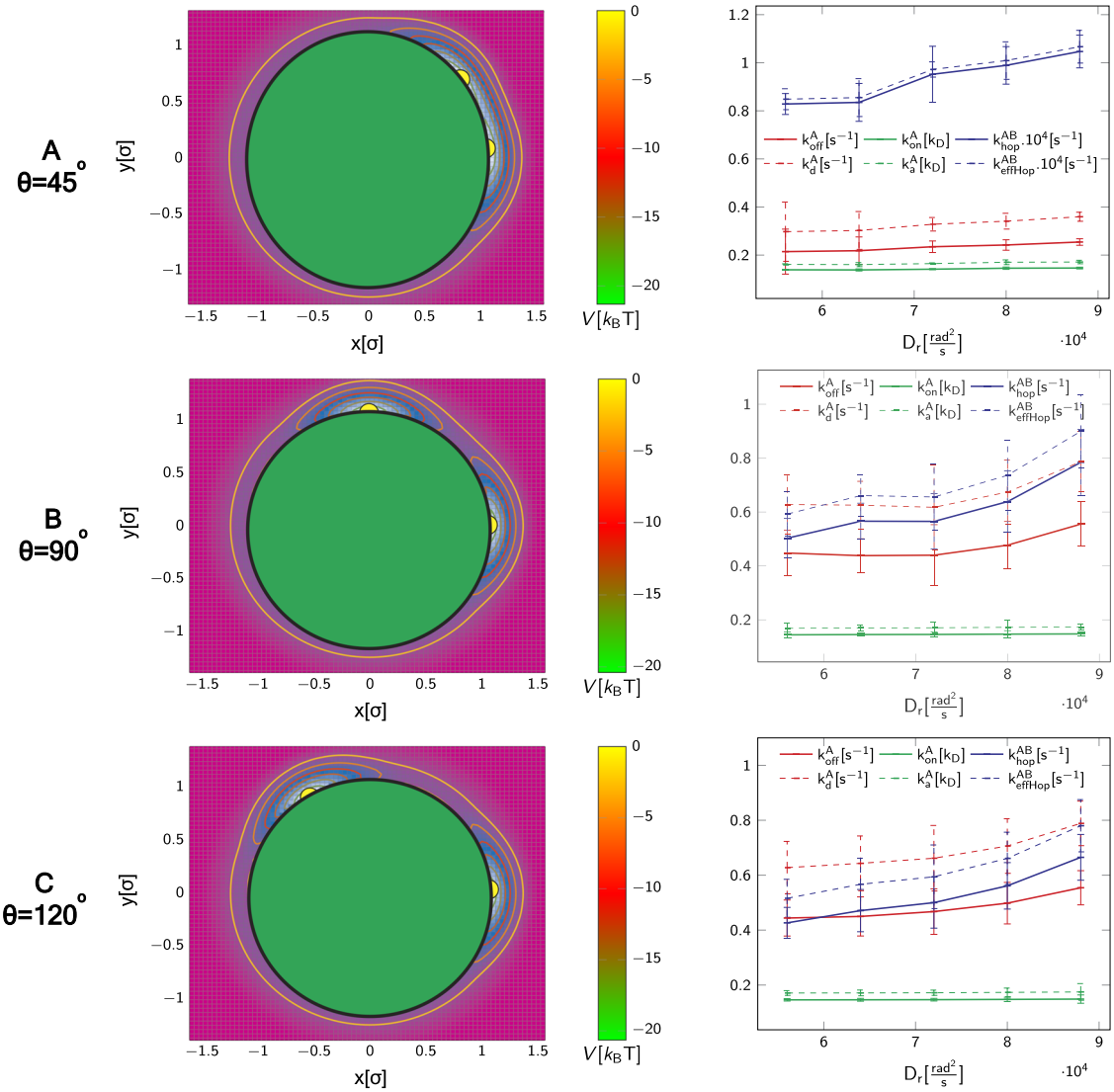

FIG. 3. Potential energy landscape (left column) of the enzyme-substrate system as a function of the spacial position of the pair and rate constants evaluated with the derived expressions (right column). The energy landscape is obtained by moving the enzyme around the substrate, with the patch of the enzyme pointed to the centre of the substrate. The rows (a), (b), and (c) correspond to a patch spacing θ (angle between the two patch vectors) of 45°, 90°, and 120°, respectively. For all three angles, all the rate constants increase as a function of the orientational diffusion constant D_r. However the hopping rate constants show the strongest dependence, while the association rate constants show the least. The hopping rate constants are largest when $\theta = 45°$ and decreases as the spacing increases. The dissociation rate constants are smallest when $\theta = 45°$ and increases when $\theta = 90°$. Furthermore, increase in the spacing between the patches has no effect on the dissociation rate constant. The association rate constants are not influenced by the patch spacing.

being on the millisecond-second time scale, are typical for biological systems.[2,51,52]

D. Simulation details

All simulations are performed using a Brownian dynamics integrator.[53] The system specific parameters of the simulation are as follows: The particle diameter is $\sigma = 5$ nm, the time step is $\delta t = 0.1$ ns, the mass of the particle is $m = 50$ kDa, the mass moment of inertia is $M = \frac{8}{15} m\sigma^2$, the translational and rotational friction coefficients are $\gamma = \frac{k_B T}{D_t m}$ and $\Gamma = \frac{k_B T}{D_r M}$, respectively, where $D_t = 1\mu\text{m}^2/\text{s}$ and D_r are translational and rotational diffusion constants, $k_B = 1.38 \times 10^{-23}$ JK^{-1} is the Boltzmann constant, and $T = 300$ K is the temperature of the system.

As we employ an anisotropic interaction potential, a geometrical definition of interfaces for FFS is not easy. Therefore, we base the interfaces on the potential energy up to the potential cutoff. The first interface (r_0-interface), which defines the bound state, is located at 18 kBT. The other interfaces are located at 15, 10, and 5 kBT. The interface at the cutoff of the potential is defined by zero energy and $R = 1.6\sigma_{an}$. Beyond the cutoff of the potential, the interfaces are defined by the interparticle distance $R = 1.7$, 1.9, 2.1, 2.3, 2.5, 3.0, 3.5, 4.0, 4.5, 5.0, 5.5. Finally the r_n-interface is located at $R = 7\sigma_{an}$.

III. RESULTS

In this section, we evaluate the transition rate constants using the expressions derived in Sec. II B for the patchy particle model system described in Sec. II C. First, we determine all rate constants for the case with the enzyme initially bound to one

of the patches of the substrate. Employing FFS on the dissociation reaction, we determine all six rate constants as a function of the rotational diffusion constant D_r for several patch angular spacings. Next, we compare the computed association and dissociation rate constants for this case to two other scenarios: (i) the other substrate patch is blocked by a static/inert (second) enzyme and (ii) the substrate has only a single patch, which is identical to the other patch being blocked by an infinitesimally small enzyme.

A. Effect of the rotational diffusion constant and patch spacing on the rate constants

From the FFS simulation of the dissociation reaction of an enzyme initially bound to a patch, we compute the association, dissociation, and hopping rate constants as a function of the rotational diffusion constant for patch opening angles 45°, 90°, and 120°. Figure 3 shows the potential energy landscapes and the rate constants resulting from Eqs. (3)–(5), (20), (25), and (24). In the system that we present here, since the substrate has two identical patches, the value of α measured from the simulation is around 0.5.

For all path opening angles, the rate constants only weakly increase as a function of the orientational diffusion constant D_r. The hopping rate constant has the strongest dependence on D_r, whereas the association rate constant has the weakest. At higher D_r, the particles rotate faster, allowing the particle to leave the potential well more easily since even a small misalignment of the patches causes unbinding. Once unbound, the particle either dissociates or hops to the other patch. Hence, the hopping and dissociation rate constants sensitively depend on D_r. The association rate constant, on the other hand, increases only marginally with D_r, as the rotational diffusion does not limit the rate constant of association for these values of D_r.

Figure 3(a) shows that for the $\theta = 45°$ case, the two patches partly overlap, enhancing the probability for hopping rather than dissociation. Hence, for $\theta = 45°$, the dissociation rate constant is lower and the hopping rate constant is four orders of magnitude larger when compared to the dissociation and the hopping rate constants when $\theta = 90°$ or $\theta = 120°$. For the higher patch angles, the two patches truly separate so that an enzyme unbinding from one patch rarely hops to the other patch. When the patch angle is increased from $\theta = 45°$ to $\theta = 90°$, the dissociation rate constant initially increases but levels off when the patches are positioned at $\theta = 120°$. Association rate constants are hardly dependent on the angular distance between the patches.

B. Effect of blocking on the rate constants

As the substrate has more than one binding site (patch), multiple enzymes can bind simultaneously. The presence of another bound enzyme might affect the association and dissociation rate constants of an enzyme to and from the free patches. Restricting ourselves to a substrate with two patches, we consider first the case where one of the two patches is blocked by an identical enzyme. We assume this enzyme to remain bound and treat it as being static and inert. In this case, the hopping rate constants are zero since the enzyme cannot hop to the other patch. We compute the effective and intrinsic association/dissociation rate constants for patch opening angles $\theta = 90°$ and $\theta = 120°$. We also compare the computed rate constants to those obtained when there is no blocking and the case where the substrate has only one patch.

Figure 4 shows the energy landscapes for $\theta = 90°$ and $\theta = 120°$, while Fig. 5 shows the intrinsic and effective association and dissociation rate constants for all cases. From the energy landscape, we see that the mobile enzyme (not shown in the figure) feels a strong specific attractive force around the free patch, a weak non-specific attractive force around the substrate, and a repulsive force near the blocking enzyme. Figure 5 shows that all rate constants increase with increasing rotational diffusion constant. The association rate constants k_a^A and k_{on}^A are highest for the one patch case and for blocked patch case with $\theta = 120°$. For the blocked patch case with

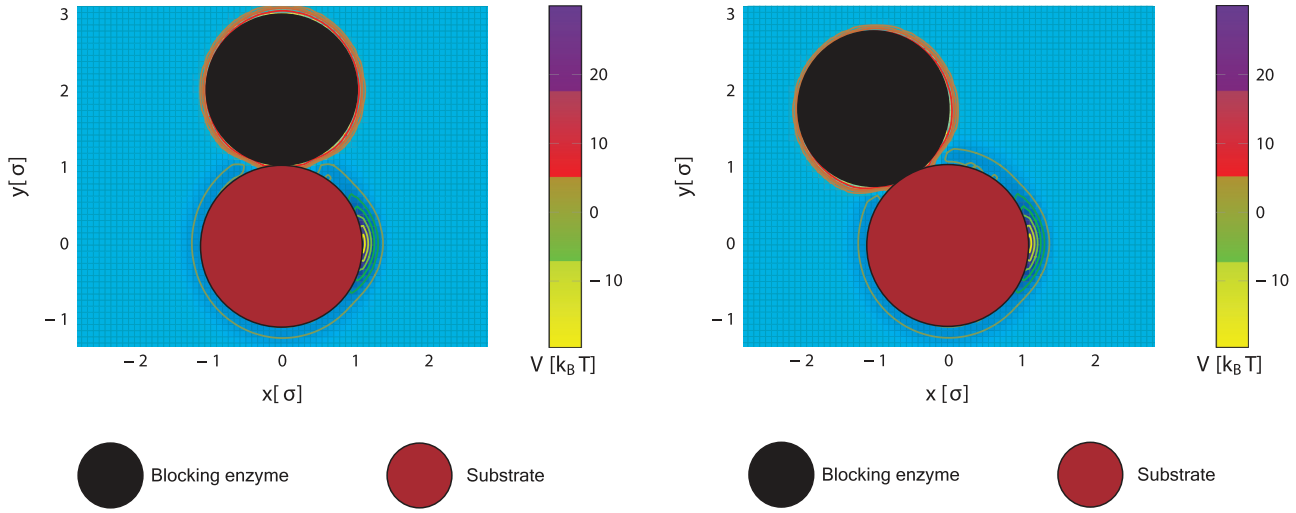

FIG. 4. Potential energy landscapes when one of the patches is blocked by an enzyme when $\theta = 90°$ (left) and $\theta = 120°$ (right). The second enzyme particle (not shown in the figure) feels a strong attraction around the free patch, a weak non-specific attraction around the substrate, and a repulsive force around the blocking enzyme.

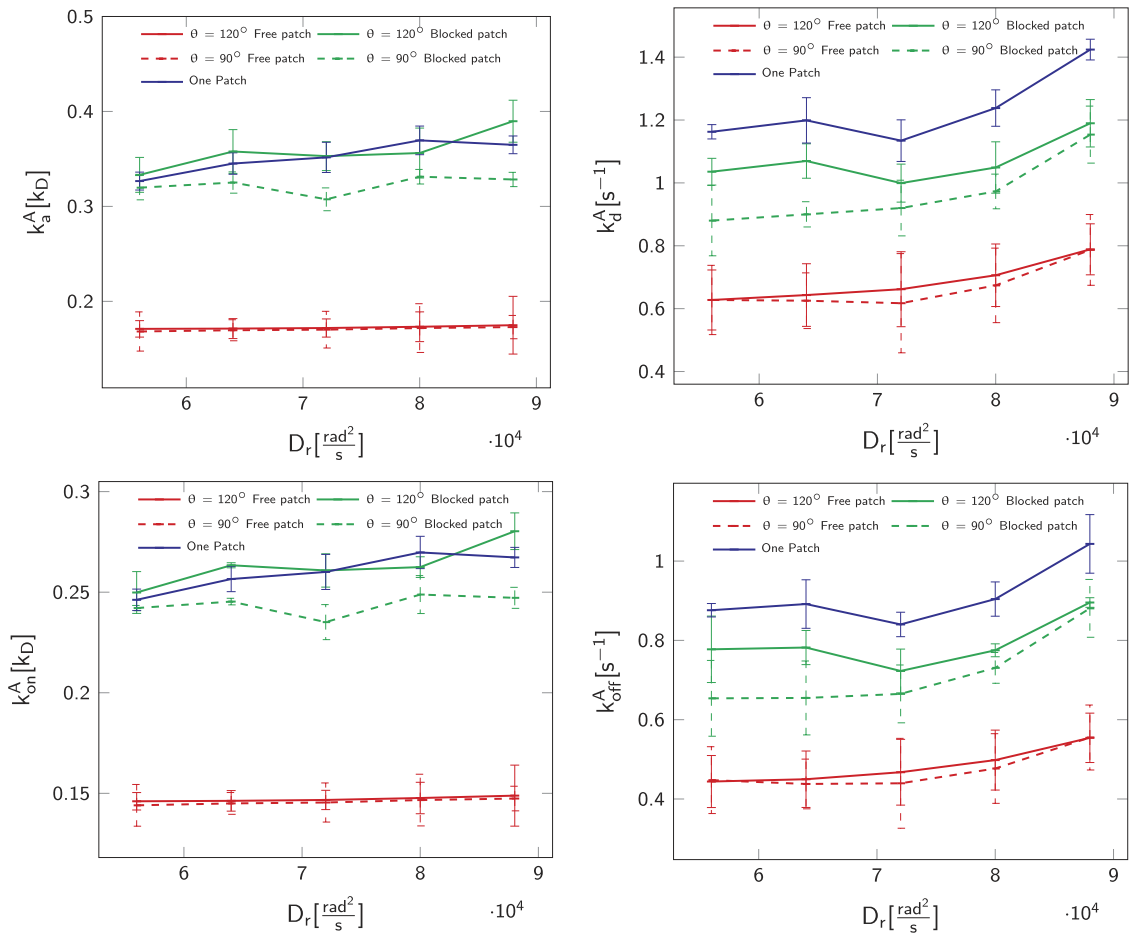

FIG. 5. Clockwise from top left: The intrinsic association rate constant, k_a, intrinsic dissociation rate constant, k_d, effective dissociation rate constant, k_{off}, and effective association rate constant, k_{on}, plotted as a function of the rotational diffusion constant, D_r, for three cases: (i) substrate with two patches and both patches are free (free patch), (ii) substrate with two patches and one of the patch is blocked, (iii) substrate with one patch. The association rate constants are largest when the substrate has one patch and when one patch is blocked with $\theta = 120°$. The association rate constants for the blocked patch when $\theta = 90°$ is lower than the above value and is least when the substrate has two patches with no blocking. The dissociation rate constant on the other hand is largest when the substrate has a single patch and least when both patches are free. When one patch is blocked, the dissociation rate constants lie in between the above values.

$\theta = 90°$, the association rate constants are slightly smaller because the blocking enzyme is closer to the free patch and causes steric hindrance, reducing the association rate constant. When the patches are further apart, this effect is reduced, corresponding to an increased association rate constant. The association rate constants are lowest for the unblocked two patch case. Since the association is specific to patch A, we do not count trajectories that bind to patch B, which acts as a trap, effectively reducing the association rate constant for binding to patch A.

The dissociation rate constants are largest for the one patch situation because once the enzyme leaves the potential well, it is only held by the weak non-specific attraction, enhancing the chance to escape. The dissociation rate constants are lowest for the unblocked two-patch case since an enzyme leaving a potential well still can hop to the other patch and rebind to the substrate, thus reducing the dissociation rate constants. The dissociation rate constants for the blocked-patch scenario are in between the two other cases, as then an enzyme leaving a potential well is repelled by the blocking enzyme and rebinds to the patch where it started from. This effect is larger for small distances between the patches, leading to smaller dissociation rate constants for $\theta = 90°$ compared to the dissociation rate constant for $\theta = 120°$.

IV. CONCLUSION

In this work, we derived a generic expression to evaluate the dissociation rate constant using FFS, for cases where two states are not necessarily separated by all interfaces. This expression is also applicable to the case of more than two states. Moreover, we derived microscopic expressions for intrinsic and effective association, dissociation, and hopping rate constants, to be used in conjunction with a single rare-event simulation of the dissociation reaction.

Because in signalling networks, the rebinding of the enzyme to the substrate can significantly change the response of the system, it is interesting to study the rate constants of binding, unbinding, and hopping (rebinding) of an enzyme to the substrate. In our model, we restrict the number of binding sites on the substrate to two and the enzyme has one binding site. For this model, we calculate the rate constants as a function of the rotational diffusion constant, D_r, and the spacing between the two patches on the surface of the

substrate. We find that the association rate constants are mostly independent of how fast the particles rotate, while the dissociation and hopping rate constants are more strongly correlated with D_r (see also Ref. 33). When the patches are close to each other, the enzyme hops (rebinds) to the other substrate patch, instead of diffusing away. This hopping rate constant depends on the patch distance very strongly. By contrast, the association and dissociation rate constants do not change significantly with patch separation. Finally, we studied the effect of a blocking enzyme on the associating/dissociation/hopping rate constants. In the presence of an (inert) blocking enzyme, both the association and dissociation rate constants increase when compared to the unblocked case. This might appear counter-intuitive at first, as blocking would seem to lower the chance of association rather than enhancing it. However, when considering binding to one specific site, the other site acts as a trap, effectively reducing this association rate[47] with respect to a single-site substrate. This reduction is less than a factor of two as the two sites together also have a larger effective cross section, which would enhance the association again. Indeed, the association rate constant to either of the two patches is larger than the association rate constant for the one-patch systems. As expected from microscopic reversibility, the second site also acts as a trap on the dissociation pathway, reducing the dissociation rate constant.[47] Removing this site by blocking thus enhances both the association and dissociation rate constants.

Evaluation of these rate constants is useful for understanding in general the association reactions in an enzyme-substrate system and to study the response characteristics of such a system. The intrinsic rate constants also serve as input parameters for a multi-scale simulation,[49,54] where, by using these rate constants, explicit simulations of the association reactions can be avoided, which dramatically speeds up the simulations.

ACKNOWLEDGMENTS

This work is part of the Industrial Partnership Programme (IPP) "Computational sciences for energy research" of the Foundation for Fundamental Research on Matter (FOM), which is financially supported by the Netherlands Organization for Scientific Research (NWO). This research programme is co-financed by Shell Global Solutions International B.V.

[1] V. Dahirel, F. Paillusson, M. Jardat, M. Barbi, and J.-M. Victor, Phys. Rev. Lett. **102**, 228101 (2009).
[2] G. Schreiber, G. Haran, and H. X. Zhou, Chem. Rev. **109**, 839 (2009).
[3] G. Schreiber, Curr. Opin. Struct. Biol. **12**, 41 (2002).
[4] R. R. Gabdoulline and R. C. Wade, J. Mol. Recognit. **12**, 226 (1999).
[5] A. C. Pan, D. W. Borhani, R. O. Dror, and D. E. Shaw, Drug Discovery Today **18**, 667 (2013).
[6] V. Vanguri, C. C. Govern, R. Smith, and E. S. Huseby, Proc. Natl. Acad. Sci. U. S. A. **110**, 288 (2013).
[7] N. Agmon and A. Szabo, J. Chem. Phys. **92**, 5270 (1990).
[8] O. G. Berg and P. H. von Hippel, Annu. Rev. Biophys. Biophys. Chem. **14**, 131 (1985).
[9] S. H. Northrup and H. P. Erickson, Proc. Natl. Acad. Sci. U. S. A. **89**, 3338 (1992).
[10] H.-X. Zhou, J. Chem. Phys. **108**, 8139 (1998).
[11] C.-Y. F. Huang and J. E. Ferrell, Jr., Proc. Natl. Acad. Sci. U. S. A. **93**, 10078 (1996).
[12] J. E. Ferrell, Jr., Trends Biochem. Sci. **21**, 460 (1996).
[13] J. E. J. Ferrell and R. R. Bhatt, J. Biol. Chem. **272**, 19008 (1997).
[14] K. Takahashi, S. Tănase-Nicola, and P. R. ten Wolde, Proc. Natl. Acad. Sci. U. S. A. **107**, 2473 (2010).
[15] I. V. Gopich and A. Szabo, Proc. Natl. Acad. Sci. U. S. A. **110**, 19784 (2013).
[16] K. Aokia, M. Yamada, K. Kunida, S. Yasuda, and M. Matsuda, Proc. Natl. Acad. Sci. U. S. A. **108**, 12675 (2011).
[17] T. E. Ouldridge and P. R. ten Wolde, Biophys. J. **107**, 2425 (2014).
[18] H. C. Berg and E. M. Purcell, Biophys. J. **20**, 193 (1977).
[19] W. Bialek and S. Setayeshgar, Proc. Natl. Acad. Sci. U. S. A. **102**, 10040 (2005).
[20] K. Wang, W.-J. Rappel, R. Kerr, and H. Levine, Phys. Rev. E **75**, 061905 (2007).
[21] A. M. Berezhkovskii and A. Szabo, J. Chem. Phys. **139**, 121910 (2013).
[22] P. R. ten Wolde, N. B. Becker, T. E. Ouldridge, and A. Mugler, J. Stat. Phys. **162**, 1395 (2016).
[23] J. S. van Zon and P. R. ten Wolde, J. Chem. Phys. **123**, 234910 (2005).
[24] M. J. Morelli and P. R. ten Wolde, J. Chem. Phys. **129**, 054112 (2008).
[25] J. Lipková, K. C. Zygalakis, S. J. Chapman, and R. Erban, J. Appl. Math. **71**, 714 (2011).
[26] M. E. Johnson and G. Hummer, Phys. Rev. X **4**, 031037 (2014).
[27] H. C. R. Klein and U. S. Schwarz, J. Chem. Phys. **140**, 184112 (2014).
[28] A. Vijaykumar, P. G. Bolhuis, and P. R. ten Wolde, Faraday Discuss. **195**, 421 (2016).
[29] T. S. van Erp, D. Moroni, and P. G. Bolhuis, J. Chem. Phys. **118**, 7762 (2003).
[30] R. J. Allen, P. B. Warren, and P. R. ten Wolde, Phys. Rev. Lett. **94**, 018104 (2005).
[31] R. J. Allen, C. Valeriani, and P. Rein ten Wolde, J. Phys.: Condens. Matter **21**, 463102 (2009).
[32] D. Fusco and P. Charbonneau, Phys. Rev. E **88**, 012721 (2013).
[33] A. C. Newton, J. Groenewold, W. K. Kegel, and P. G. Bolhuis, Proc. Natl. Acad. Sci. U. S. A. **112**, 15308 (2015).
[34] C. Gögelein, G. Nägele, R. Tuinier, T. Gibaud, A. Stradner, and P. Schurtenberger, J. Chem. Phys. **129**, 085102 (2008).
[35] A. W. Wilber, J. P. K. Doye, A. A. Louis, and A. C. F. Lewis, J. Chem. Phys. **131**, 175102 (2009).
[36] M. G. Noro and D. Frenkel, J. Chem. Phys. **113**, 2941 (2000).
[37] G. Foffi and F. Sciortino, J. Phys. Chem. B **111**, 9702 (2007).
[38] Y. Wang, Y. Wang, D. R. Breed, V. N. Manoharan, L. Feng, A. D. Hollingsworth, M. Weck, and D. J. Pine, Nature **491**, 51 (2012).
[39] D. J. Kraft, R. Ni, F. Smallenburg, M. Hermes, K. Yoon, D. A. Weitz, A. van Blaaderen, J. Groenewold, M. Dijkstra, and W. K. Kegel, Proc. Natl. Acad. Sci. U. S. A. **109**, 10787 (2012).
[40] G. Odriozola and M. Lozada-Cassou, Phys. Rev. Lett. **110**, 105701 (2013).
[41] L. Colón-Meléndez, D. J. Beltran-Villegas, G. van Anders, J. Liu, M. Spellings, S. Sacanna, D. J. Pine, S. C. Glotzer, R. G. Larson, and M. J. Solomon, J. Chem. Phys. **142**, 174909 (2015).
[42] E. Bianchi, R. Blaak, and C. N. Likos, Phys. Chem. Chem. Phys. **13**, 6397 (2011).
[43] E. Jankowski and S. C. Glotzer, Soft Matter **8**, 2852 (2012).
[44] A. C. Newton, J. Groenewold, W. K. Kegel, and P. G. Bolhuis, J. Chem. Phys. **146**, 234901 (2017).
[45] Y. Y. Kuttner, N. Kozer, E. Segal, G. Schreiber, and G. Haran, J. Am. Chem. Soc. **127**, 15138 (2005).
[46] C. Li, Y. Wang, and G. J. Pielak, J. Phys. Chem. B **113**, 13390 (2009).
[47] A. C. Newton, R. Kools, D. W. H. Swenson, and P. G. Bolhuis, J. Chem. Phys. **147**, 155101 (2017).
[48] W. Du and P. G. Bolhuis, J. Chem. Phys. **140**, 195102 (2014).
[49] A. Vijaykumar, T. E. Ouldridge, P. R. ten Wolde, and P. G. Bolhuis, J. Chem. Phys. **146**, 114106 (2017).
[50] A. Vijaykumar, P. R. ten Wolde, and P. G. Bolhuis, J. Chem. Phys. **147**, 184108 (2017).
[51] R. Milo, P. Jorgensen, U. Moran, G. Weber, and M. Springer, Nucl. Acids Res. **38**, D750 (2009).
[52] See bionumbers.hms.harvard.edu for information about dissociation and association rate constants in biological systems.
[53] R. Davidchack, T. Ouldridge, and M. Tretyakov, J. Chem. Phys. **142**, 144114 (2015).
[54] A. Vijaykumar, P. G. Bolhuis, and P. R. ten Wolde, J. Chem. Phys. **143**, 214102 (2015).